Chemistry & Biology
Article

Insights into Bacterial 6-Methylsalicylic Acid Synthase and Its Engineering to Orsellinic Acid Synthase for Spirotetronate Generation

Wei Ding,[1,2] Chun Lei,[1] Qingli He,[1] Qinglin Zhang,[1] Yurong Bi,[2] and Wen Liu[1,*]
[1]State Key Laboratory of Bioorganic and Natural Products Chemistry, Shanghai Institute of Organic Chemistry, Chinese Academy of Sciences, 345 Lingling Road, Shanghai 200032, China
[2]School of Life Science, Lanzhou University, 222 South Tianshui Road, Lanzhou 730000, China
*Correspondence: wliu@mail.sioc.ac.cn
DOI 10.1016/j.chembiol.2010.04.009

SUMMARY

The enzymes 6-methylsalicylic acid (6-MSA) synthases (6-MSASs) are involved in the building of an aryl moiety in many bioactive secondary metabolites produced by fungi and bacteria. Using the bacterial 6-MSAS ChlB1 in the biosynthesis of spirotetronate antibiotic chlorothricin (CHL) as a model, functional analysis of its dehydratase (DH) and ketoreductase (KR) domains by site-specific mutagenesis revealed that selective ketoreduction is not essential for polyketide chain extension. Promiscuity of the ketoacylsynthase domain in β functionality recognition allows for engineering ChlB1 to an orsellinic acid (OSA) synthase (OSAS) by inactivating KR at the active site. The engineered ChlB1 is compatible with the enzymes for late-stage tailoring in CHL biosynthesis, featuring specific protein recognitions that facilitate variable aryl group incorporation. The resulting spirotetronates, which bear an OSA-derived aryl group, exhibited antibacterial activities comparable to those of the parent products.

INTRODUCTION

The enzymes 6-methylsalicylic acid (6-MSA) synthases (6-MSASs) belong to a class of polyketide synthases (PKSs) that are structurally type I but act iteratively for aromatic polyketide biosynthesis (Fujii, 1999; Shen, 2000; Hertweck, 2009). They consist of multiple functional domains, including the ketoacylsynthase (KS), acyltransferase (AT), dehydratase (DH), ketoreductase (KR), and acyl carrier protein (ACP) on a single protein (Figure 1A). In a process resembling fatty acid biosynthesis, 6-MSASs catalyze the assembly of a nascent tetraketide from one acetyl-CoA and three malonyl-CoAs by successive decarboxylative condensations. However, they clearly differ from fatty acid synthases in processing the β-oxo functionality and furnishing the product (Figure 1B), as (1) the KR domain selectively reduces the β-keto group only on the growing triketide intermediate **1** to give **2**, followed by the cognate DH domain-catalyzed dehydration to form a double bond of **3**; and (2) the tetraketide intermediate **4** undergoes intramolecular aldol condensation, dehydration, and aromatization to afford 6-MSA.

Fungal 6-MSASs, along with other iterative PKS model systems such as the nonreducing PksA in aflatoxin biosynthesis (Crawford et al., 2008, 2009) and highly reducing LovB in lovastatin biosynthesis (Kennedy et al., 1999; Ma et al., 2009), have been extensively investigated to access the mechanisms for chain-length control, regiospecific reduction, substrate tolerance, and subunit-domain interaction (Dimroth et al., 1976; Beck et al., 1990; Spencer and Jordan, 1992; Bedford et al., 1995; Fujii et al., 1996; Kealey et al., 1998; Richardson et al., 1999; Moriguchi et al., 2006, 2008). Recently, 6-MSASs have been widely found in bacteria, such as ChlB1 from *Streptomyces antibioticus* (Jia et al., 2006; Shao et al., 2006), MdpB from *Actinomadura madurae* (Van Lanen et al., 2007), PokM1 from *S. diastatochromogenes* (Daum et al., 2009), and PtmQ from *S. pactum* (Ito et al., 2009), and are involved in the incorporation of a 6-MSA derivative moiety into a number of structurally diverse, bioactive secondary metabolites (see Figure S1A available online). Fungal and bacterial 6-MSASs share high homologies in sequence and domain organization, suggesting their relationship in evolution (Figure S1B). Previous biochemical studies on fungal 6-MSASs confirmed their KR domain function: the native protein in the absence of NADPH or the KR mutant enzyme with the inactivated NADPH binding site synthesizes a shunt triketide compound (Figure 1B), triacetic acid lactone (TAL), indicating the selective action of the KR domain for reducing the β-keto group of the intermediate **1**. However, it is inconclusive whether **1** has to be reduced before reacting with the third malonyl-CoA for proceeding further, despite no tetraketide compound being identified. The reductive control in polyketide chain elongation is not stringent for reactions catalyzed by noniterative type I PKSs, as alterations of β-keto functionalities can often be achieved on polyketides by modulating the activity of the KR, DH, or enoylreductase (ER) domain in modules during the growing process (McDaniel et al., 2005). Similar to this, orsellinic acid (OSA) biosynthesis in bacteria, also catalyzed by iterative type I PKSs, requires no reduction step in the process of tetraketide intermediate (**6**) assembly (Figure 1B). OSA synthases (OSASs), including AviM in avilamycin biosynthesis (Gaisser et al., 1997) and CalO5 in calicheamicin biosynthesis (Figure S1) (Ahlert et al., 2002), are composed of the KS, AT, DH, and ACP domains (Figure 1A), displaying a head-to-tail homology to 6-MSASs with the only exception of the omission

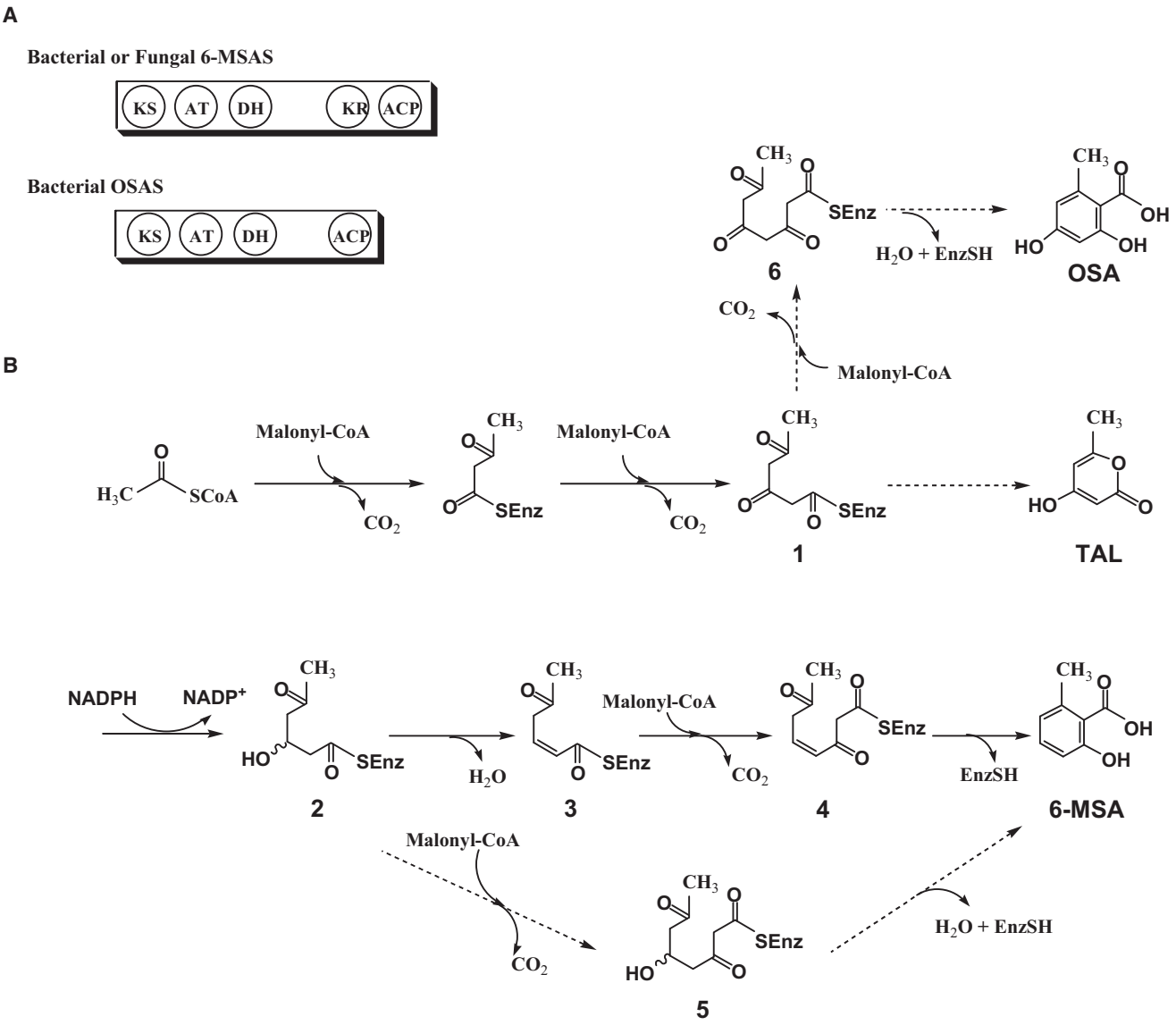

Figure 1. 6-Methylsalicylic Acid Synthase and Orsellinic Acid Synthase, and Biosyntheses of 6-MSA, Triacetic Acid Lactone, and Orsellinic Acid

(A) Domain organizations of 6-methylsalicylic acid synthase (6-MSAS) and orsellinic acid synthase (OSAS). KS, ketoacylsynthase; AT, acyltransferase; DH, dehydratase; KR, ketoreductase; ACP, acyl carrier protein.

(B) Pathways for 6-MSA synthesized by 6-MSASs and DH mutant ChlB1 (H947F), for triacetic acid lactone (TAL) synthesized by KR-mutated fungal 6-MSASs (AxPxxA at the NADPH binding site), and for orsellinic acid (OSA) synthesized by OSASs AviM, CalO5, and KR-mutated ChlB1 (Y1450F at the active site). For 6-MSASs, solid arrows indicate native enzyme-catalyzed reactions, and dashed arrows showed the shunt reactions catalyzed by mutant enzymes.

of the KR domain. This implies that KR-catalyzed reduction for iterative type I PKSs in aromatic polyketide biosynthesis may not be essential for polyketide chain extending, but remains to be confirmed experimentally.

Incorporation of the 6-MSA moiety into natural products requires pathway-specific enzymes for PKS postmodification and incorporation. We have recently dissected two distinct acyltransfer reactions centered on the acyl-*S*-ACP intermediate for introducing the 6-MSA moiety to the biosynthesis of spirotetronate antibiotic chlorothricin (CHL) (He et al., 2009). The 6-MSA moiety from the 6-MSAS ChlB1 is transferred by the first AT ChlB3 onto the discrete ACP ChlB2, which may serve as a platform for *O*-methylation and optional chlorination, and is then appended to the terminal D-olivose unit by the second AT ChlB6 (see below). Given that the ACP-mediated strategy commonly facilitates the molecular recognition of downstream enzymes (Freitag et al., 2005; Van Lanen et al., 2005; Singh et al., 2007; Balibar et al., 2007; Fridman et al., 2007; Heide, 2009), the ACP-tethered, diverse aryl groups (2-methoxy-6-methyl-benzoyl and its 5-chlorinated derivative) are readily transferred and incorporated into the final molecule to afford deschloro-CHL and CHL, respectively. The advantage of effective

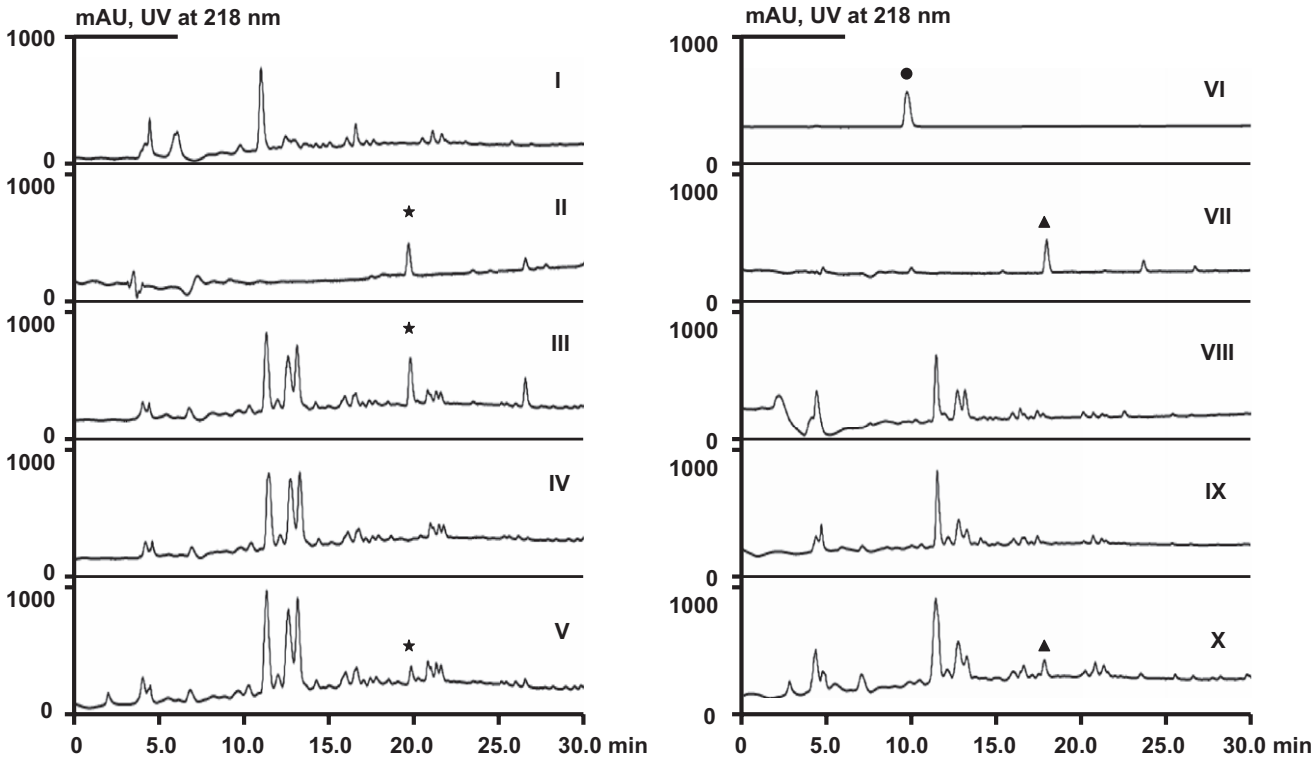

Figure 2. Functional Validation of DH or KR Mutant ChlB1 Derivatives in *S. albus*

HPLC analysis of the products from the negative control TL1006 (carrying the vector pTGV-2) (I); standard 6-MSA (II, asterisk); TL1071 for the native ChlB1 (III); TL1072 for the DH mutant with H947A (IV); TL1073 for the DH mutant with H947F (V); standard TAL (VI, dot); standard OSA (VII, triangle); TL1074 for the KR mutant with G1389A (VIII); TL1075 for the KR mutant with G1387A, G1389P, and G1392A (XI); and TL1076 for the KR mutant with Y1540F (X).

protein-protein interactions can be taken to alter the aryl functionality for structural diversity.

Here, upon investigation into the functions of the DH and KR domains by using the bacterial 6-MSAS ChlB1 as a model, we report success in the engineering of this iterative type I PKS into an OSAS by inactivating KR at the active site and show the dispensability of the selective ketoreduction in polyketide chain extending. More excitingly, this engineered ChlB1 for OSA biosynthesis can effectively collaborate with downstream enzymes in the CHL biosynthetic pathway, allowing for the altered aryl moiety transfers and modifications to generate new spirotetronates which showed biological activities at least comparable to those of the parent compounds CHL and deschloro-CHL.

RESULTS AND DISCUSSION

Heterologous Expression of *chlB1* in *Streptomyces albus* for 6-MSA Production

We first developed an approach to investigate in vivo the domain functions of bacterial 6-MSAS by heterologous expression of *chlB1* in *S. albus*. Although 6-MSA production was previously detected by expressing *chlB1* in *S. lividans* (Shao et al., 2006), the poor yield (0.2–0.4 mg/L) may largely impede progress for identifying the putative products of mutant ChlB1 derivatives in this host system. The DNA fragments encoding the functional domain(s) (i.e., KS, AT, DH, and KR-ACP) were individually amplified by PCR. After sequencing to confirm the fidelity, we assembled these fragments in *chlB1* under the control of the constitutive promoter *PermE**. The strategy used here facilitates the introduction of site-specific mutations into the target domain of ChlB1. Further introduction of the resulting construct into *S. albus* was carried out, giving the recombinant strain TL1071 for product detection along with the control *S. albus* strain AL1006 that carries the vector pTGV2 (Zhao et al., 2008). HPLC-MS analysis showed that TL1071 produces 6-MSA (Figure 2, III), with an improved yield of ≈2.0 mg/L. Consistent with our previous finding, the 6-MSA moiety synthesized by ChlB1 is readily hydrolyzed to give the free acid without functional association of downstream enzymes for transfer (Shao et al., 2006). This method was therefore applied in the following studies to probe the activities of the DH and KR domains of ChlB1.

Effects of DH Domain Inactivation on 6-MSA Production

Sequence alignment of ChlB1 with various iterative type I PKSs revealed a highly conserved motif in the DH domain, HxxxGxxxxP, in which the His residue, corresponding to His947 of ChlB1, is located at the active site (Figure S1B) (Aparicio et al., 1996). To inactivate the DH domain of ChlB1, we replaced His947 by site-specific mutagenesis with Ala and Phe, according to the strategies previously used for functional studies of the iterative fungal 6-MSAS ATX and the noniterative PKS in picromycin biosynthesis (Wu et al., 2005; Moriguchi

et al., 2008). The constructs were then introduced into *S. albus*, yielding the recombinant strains TL1072 (for H947A substitution) and TL1073 (for H947F substitution). Similar to that observed from the corresponding H939A DH mutant ATX, the mutation of H947A in ChlB1 completely abolished 6-MSA production in TL1072 (Figure 2, IV). Interestingly, TL1073, harboring the construct for expressing the H947F DH mutant ChlB1, still produced 6-MSA with a yield of ≈0.4 mg/L (Figure 2, V), approximately one fifth that produced by TL1071. The decrease in enzymatic activity of DH cannot be excluded in this H947F mutation; alternatively, this finding indicates that the dehydration activity of the ChlB1-DH domain is important but may not be indispensable for producing 6-MSA, given that the proposed tetraketide intermediate **5** could undergo an intramolecular cyclization followed by spontaneous dehydrations to furnish the relatively stable aromatic compound 6-MSA (Figure 1B). If so, H947A substitution may significantly change a certain conformation of the protein for display of enzymatic activity.

Effects of KR Domain Inactivation on Polyketide Chain Elongation

We initially chose to mutate the NADPH binding site of the ChlB1-KR domain, which features a highly conserved GxGxxG motif in the well-known Rossmann fold (Figure S1B) (Chen et al., 1990; Rescigno and Perham, 1994). This motif was replaced via a single substitution of the second Gly residue (corresponding to Gly1389) to give GxAxxG, or via triple substitution of all three Gly residues (corresponding to Gly1387, Gly1389, and Gly1392) to yield AxPxxA, as previously used in the functional analysis of fungal 6-MSASs by site-specific mutagenesis (Richardson et al., 1999; Moriguchi et al., 2008). These replacements resulted in the complete abolition of 6-MSA production in the recombinant strains TL1074 (for GxAxxG mutation of ChlB1) and TL1075 (for AxPxxA mutation of ChlB1) (Figure 2, VIII and IX, respectively), consistent with findings in the studies of fungal 6-MSASs. TAL was not detectable in either strain, although this shunt triketide product had been seen in the mutated fungal 6-MSASs. The polyketide nonproducing fact could be simply referred to as binding of the cofactor NADPH may be necessary for the enzyme to maintain an active conformation. To avoid such a potential change of protein without NADPH binding, we then chose to mutate the highly conserved Tyr residue (corresponding to Tyr1540 of ChlB1), which is located at the active site of the KR domain, for forming a catalytic triad along with the Lys and Ser residues (Figure S1B) (Reid et al., 2003; Caffrey, 2003; Wu et al., 2005). The same mutation has been conducted to eliminate the KR activity of module 6 of the type I noniterative PKS 6-deoxyerythronolide B (DEB) synthase, showing that further tailoring of the polyketide intermediate proceeds to afford the 3-keto derivative of DEB (Reid et al., 2003). Intriguingly, Y1540F substitution in ChlB1 led to the accumulation of a distinct product (~0.4 mg/L, comparable to that of 6-MSA production of TL1073) in the recombinant strain TL1076 (Figure 2, X). This compound is identical to OSA, supported by high-resolution electron impact mass spectrometry (HR-EI-MS) analysis (M^+ ion at *m/z* = 168.0424, 168.0423 calculated) and using an authentic compound as the standard. These findings confirmed the selective reduction activity of the ChlB1-KR domain and, more importantly, indicated that the third extending step indeed proceeds on the unreduced triketide intermediate **1** to yield **6** (Figure 1B), followed by cyclization, dehydration, and aromatization to give the final product as OSA which bears an additional C-4 hydroxyl group in comparison to 6-MSA.

For bacterial iterative type I PKSs in aromatic polyketide formation, we have proposed the catalytic nature of their KR-DH pairs (Shao et al., 2006; Zhao et al., 2008). According to a model for predicting the geometry of double bonds in polyketide intermediates, *cis* double bonds arise from L-hydroxyacyl precursors (Wu et al., 2005; Keatinge-Clay, 2007). Because the ChlB1-KR domain lacks the His residue at the active site and the characteristic L-D-D motif, ketoreduction is predicted to yield the L-hydroxyacyl intermediate (**2**) (Keatinge-Clay, 2007). The *cis* double bond could then be formed by the paired DH domain, facilitating the folding of the polyketide intermediate **4** to furnish the cyclic structure by aldol condensation (Figure 1B). The ChlB1 mutant lacking DH or KR activity retains the ability to extend the intermediate to a tetraketide (**5** or **6**), showing that the KS domain is indiscriminate in β functionality recognition because variable triketides (**2**, **3**, and **6**) can serve as substrates; but without structural constraint of the *cis* double bond, the resulting hydroxyl- or oxo-acyl backbone might be flexible, disfavoring folding and production. The yields of 6-MSA and OSA decrease to a similar level (≈0.4 mg/L) in the strains for expressing active DH-mutated ChlB1 (H947F) and KR-mutated ChlB1 (Y1540F), respectively, consistent with this prediction. Functional analysis of the DH and KR activities of ChlB1 supports a common paradigm for 6-MSA biosynthesis in bacteria and fungi, although OSA production has not been validated by inactivating the KR domain of fungal 6-MSAS at the active site.

Replacement of 6-MSAS by OSAS in the CHL Biosynthetic Pathway for New Spirotetronate Antibiotic Production

We have inactivated *chlB1* by gene replacement and identified the intermediate as DM-CHL (lacking the 6-MSA derivative moiety) (Figure 3) from the mutant strain TL1012 (Jia et al., 2006; Shao et al., 2006). Introduction of an intact *chlB1* into TL1012 was also carried out, leading to the conversion of DM-CHL to CHL. Using this well-established in *trans* complementation system, we investigated whether the variable aryl moiety can be transferred, modified, and eventually appended to DM-CHL to make new spirotetronates. The construct that encodes the engineered ChlB1 with Y1450F for OSA biosynthesis was introduced into TL1012, giving the recombinant strain TL1077 for product examination. HPLC-MS analysis of the crude extract from 25 L of solid fermentation culture revealed two distinct products, **7** and **8** (Figure 4, III), which exhibit ultraviolet absorption patterns quite similar to those of deschloro-CHL and CHL (Figure S3A). For structural elucidation, compounds **7** and **8** were purified and subjected to comparative spectroscopic analysis with the parent compound CHL. High-resolution electrospray mass spectrometry (HR-ESI-MS) analysis established the molecular formulae as $C_{50}H_{64}O_{17}$ for **7** (with the positive $[M + Na]^+$ ion at *m/z* = 959.40358, 959.40412 calculated) and $C_{50}H_{63}O_{17}Cl$ for **8** (with the positive $[M + Na]^+$ ion at *m/z* = 993.36460, 993.36515 calculated), and ESI-MS-MS analysis then narrowed their differences from CHL to the aryl groups

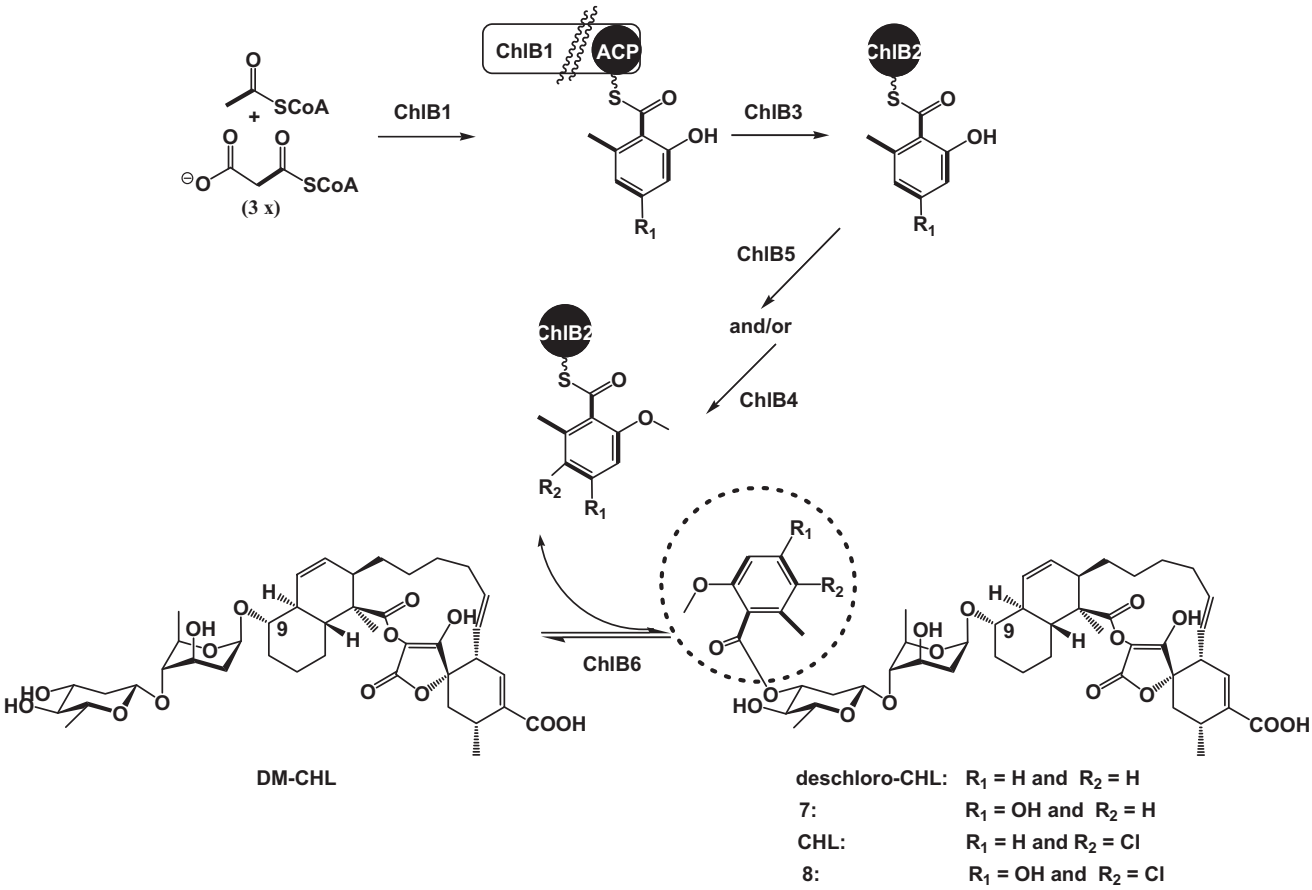

Figure 3. Aryl Group Formation and Incorporation in CHL Biosynthesis

ChlB1 or its KR mutant (Y1540F) postmodifications of the 6-MSA or OSA moiety and its transfer to DM-CHL for affording deschloro-CHL and CHL or the corresponding analogs **7** and **8**. The dashed circle indicates the variable aryl group.

(Figure S3B). For compound **7**, the ^{1}H NMR spectrum displayed two broad singlet aromatic protons at δ 6.24 and 6.29, distinct from the pair of *ortho* protons at δ 6.76 and 7.37 (d, J = 8.9 Hz) in that of CHL (Figure S3C); and the HMBC spectrum showed cross-peaks from δ 3.74 (s, CH_3-9′) to C-2′, from δ 6.29 (brs, H-3′) to C-1′, C-2′, and C-4′, from δ 6.24 (brs, H-5′) to C-4′ and C-6′, and from δ 2.23 (s, CH_3-8′) to C-1′, C-5′, and C-6′ (Figure S3E). Together with its ^{13}C NMR, ^{1}H-^{1}H COSY, HSQC, and ROESY spectra (Figures S3D and S3E), **7** was confirmed to be a new deschloro-CHL derivative, which bears a 4-hydroxylated aryl group originated from the OSA moiety (Figure 5). Similar experiments were performed for compound **8**, and the key HMBC correlations established that it is a new CHL analog possessing a 5-chlorinated OSA derivative moiety as 2-methoxy-4-hydroxy-5-chloro-6-methyl-benzoyl (Figure 5; Figures S3C and S3F).

Identification of new spirotetronates **7** and **8** in TL1077 is well in agreement with the fact that deschloro-CHL and CHL are normally coproduced by the *S. antibioticus* wild-type strain (Keller-Schierlein et al., 1969). It is remarkable, and indicative of the effective collaboration of the KR mutant ChlB1 (Y1450F) with downstream enzymes in the CHL biosynthetic pathway. The conversion of DM-CHL to **7** or **8** requires *O*-methylation (catalyzed by ChlB5) and/or chlorination (catalyzed by ChlB4) to functionalize the OSA moiety, as well as two acyltransfer steps (catalyzed by ChlB3 and ChlB6, respectively) in the process of its incorporation (Figure 3) (He et al., 2009). These reactions are strongly dependent on the specific recognitions of the proteins. Given that the discrete ACP ChlB2 provides the structural features in molecular recognition of the following enzymes (i.e., ChlB4, ChlB5, and ChlB6), the potential steric hindrance, from the additional C-4 hydroxyl group of the OSA moiety, could be attenuated. ChlB1 postmodifications (i.e., C-2 *O*-methylation and C-5 chlorination) then take place on OSA-*S*-ChlB2 for maturation, followed by the action of the second AT ChlB6 for appending the modified OSA moiety onto DM-CHL. Therefore, the engineered ChlB1 (Y1540F) should retain the ability, most likely by its ACP domain, to interact with the first AT ChlB3, allowing the transfer of the OSA moiety onto ChlB2 for tailoring.

To support this hypothesis, we introduced MSS4.3, a bacterial OSAS AviM-encoding construct (Gaisser et al., 1997), into TL1012 to generate the recombinant strain TL1078 for compound **7** and **8** examination. Because of the presence of *aviN* (in the *avi* gene cluster) encoding putative AT that is highly homologous to ChlB3 or ChlB6, the resulting OSA moiety from AviM was speculated to be directly transferred from the

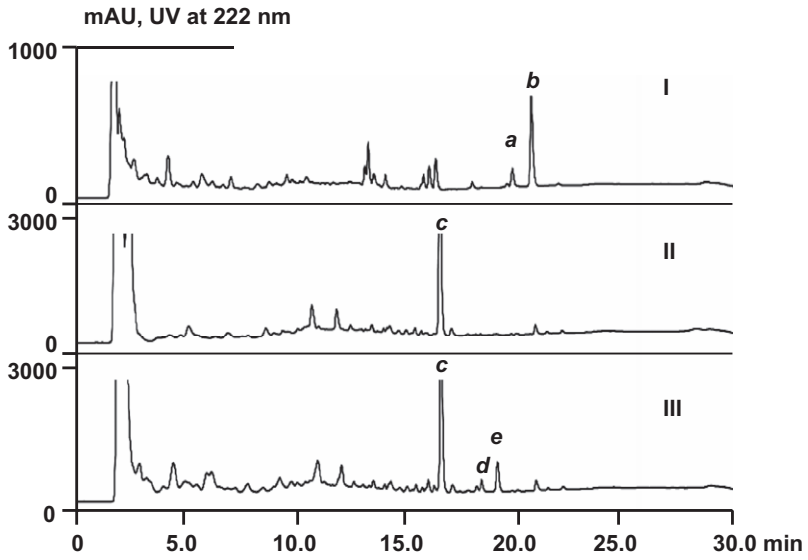

Figure 4. Validation of New Spirotetronate Production in *S. antibioticus*

HPLC analysis of fermentation cultures from the wild-type strain (I), *chlB1*-inactivated mutant TL1012 (II), and TL1077 by in *trans* complementation of the construct for expressing the KR mutant ChlB1 (Y1540F) in TL1012 (III). *a*, deschloro-CHL; *b*, CHL; *c*, DM-CHL; *d*, compound **7**; and *e*, compound **8**.

AviM-ACP domain to the molecule in avilamycin biosynthesis (He et al., 2009). The AviM-ACP-tethered acyl group can be hydrolyzed without the functional association of AviN, consistent with the fact that heterologous expression of MSS4.3 in *S. coelicolor* or *S. lividans* led to the production of the free acid OSA. TL1078 indeed accumulated OSA (Figure S2A), confirming that AviM is functional in this *S. antibioticus* strain; however, only traces (optically invisible) of compounds **7** and **8** were detected upon HPLC-MS analysis (Figure S2B), indicating the inefficient incorporation of the AviM-synthesized OSA moiety. This might be due to the unfavorable recognition between AviM-ACP and the first AT ChlB3, which does not facilitate OSA-*S*-ChlB2 generation for proceeding. These findings give new insights into aryl group formation in CHL biosynthesis, setting the stage for further engineering of the CHL biosynthetic pathway to furnish variable aryl functionality.

Bioassay of New Spirotetronates 7 and 8

To evaluate the effect of substitution of the 6-MSA derivative moiety with the OSA derivative moiety, newly obtained compounds **7** and **8** were subjected to bioassay against the Gram-positive test strains *Bacillus subtilis* and *Staphylococcus aureus*, with the parent products deschloro-CHL and CHL as controls. Although *B. subtilis* was more sensitive to the test compounds than *S. aureus* (Figure S4), compounds **7** and **8** were apparently bioactive and showed improved antibacterial activities in comparison to those of deschloro-CHL and CHL (Table 1), respectively. CHL has been previously found to be active against Gram-positive bacteria and fungi, and to inhibit cholesterol biosynthesis in rat liver homogenate via the mevalonate pathway along with its derivatives (Schindler and Zähner, 1972; Kawashima et al., 1992; Terekhova et al., 2008). The complete lack of the aryl group (to give DM-CHL) led to dramatic decreases in antibacterial activity (Jia et al., 2006). Introduction of a C-4 hydroxyl group to this aryl moiety may at least improve water solubility, which is of importance to the bioavailability of chemotherapeutic agents in vivo.

SIGNIFICANCE

The complexity of architectures of many natural products poses a tremendous challenge to chemical synthesis for

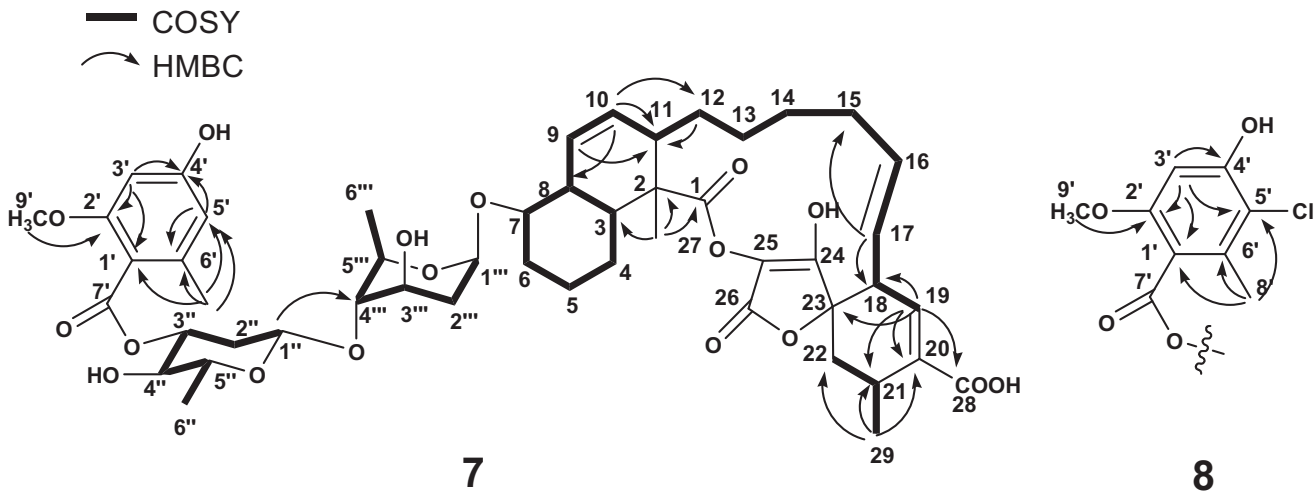

Figure 5. Structural Elucidation of New Spirotetronates

^{1}H-^{1}H COSY (for **7**) and selected HMBC correlations (for **7** and **8**) that establish the variable substitutions on the aryl group of new spirotetronates.

Table 1. Minimum Inhibitory Concentrations of Test Spirotetronates in This Study

Organism	Number[a]	MIC (μg/ml) 8	CHL	7	Deschloro-CHL
Bacillus subtilis	SIPI-JD1001	16	32	32	64
Staphylococcus aureus	SIPI-JD1002	64	128	128	>128

[a] The test organisms were deposited at the Shanghai Institute of Pharmaceutical Industry (SIPI) with the given numbers.

structural diversity. In this study, we have provided a genetic way for alteration of the aryl functionality on the complex spirotetronate antibiotic CHL, based on in vivo investigation into the functions of the KR and DH domains of the bacterial 6-MSAS ChlB1 and its compatibility with downstream enzymes for aryl moiety modification and incorporation. Our findings support a common paradigm for 6-MSA biosynthesis in bacteria and fungi, and unveil new insights into the process of aryl group formation that involves specific protein recognitions in CHL biosynthesis. KR-catalyzed selective reduction of ChlB1 is not essential for the third two-carbon unit extension to give the tetraketide intermediate. Given that triketides variable in β functionality can serve as the substrate, the promiscuity of the KS domain of ChlB1 led to the creation of a mutant for OSA biosynthesis by replacing the key amino acid residue Tyr1450 with Phe at the active site of the KR domain. Importantly, this engineered ChlB1 is compatible with downstream enzymes for late-stage tailoring, and their functional association allows for further modifications of the OSA moiety and its transfers onto the molecule, yielding the new CHL analogs 7 and 8 bearing the aryl group derived from OSA. The employed ACP-centered strategy may facilitate specific protein-protein interactions in the process. The newly obtained spirotetronates 7 and 8 exhibit antibacterial activities, which are comparable to, if not greater than, those of the parent products deschloro-CHL and CHL. Incarnating the significance of combinatorial biosynthesis methods, structural alteration of complex natural products with densely assembled functionalities (e.g., spirotetronates) can be achieved by genetic manipulation of their biosynthetic pathways.

EXPERIMENTAL PROCEDURES

Bacterial Strains, Plasmids, and Reagents

Bacterial strains and plasmids used in this study are summarized in Table S1. Biochemicals, chemicals, media, restriction enzymes, and other molecular biological reagents were purchased from standard commercial sources unless otherwise stated.

DNA Isolation, Manipulation, and Sequencing

DNA isolation and manipulation in *Escherichia coli* and *Streptomyces* were carried out according to standard methods (Kieser et al., 2000; Sambrook and Russell, 2001). PCR amplifications were carried out on an Authorized Thermal Cycler (Eppendorf AG 22331) using either *Taq* DNA polymerase or PfuUltra High-Fidelity DNA polymerase (Promega). Primer synthesis and DNA sequencing were performed at Shanghai Invitrogen Biotech and the Chinese National Human Genome Center.

Sequence Analysis

The open reading frames were deduced from the sequence by using the FramePlot 4.0beta program (http://nocardia.nih.go.jp/fp4). The corresponding deduced proteins were compared with other known proteins in the databases by available BLAST methods (http://www.ncbi.nlm.nih.gov/blast). Amino acid sequence alignment was performed by the CLUSTALW method, and the DRAWTREE and DRAWGRAM methods from BiologyWorkbench 3.2 software (http://workbench.sdsc.edu).

Heterogeneous Expression of *chlB1* and Its Derivatives in *S. albus*

To make the *chlB1* expression construct, the DNA fragments encoding individual functional domains of ChlB1 were amplified by PCR, sequenced to confirm the fidelity, and assembled by using a multiple-fragment ligation strategy. A 1.5 kb PCR product encoding the KS domain was obtained by using the primers 5′-AT GAA TTC TCT AGA GGC AGC ACC CAC GTT CTG-3′ (XbaI site underlined) and 5′-TA TAT AAG CTT AAG GGG AAC AGC CGC TCC GTC-3′ (AflII site underlined) and cloned into pSP72, yielding pAL1081; a 1.2 kb PCR product encoding the AT domain was obtained by using the primers 5′-TA GAA TTC CTT AAG CGG TGG AAC GCA GGC CGG-3′ (AflII site underlined) and 5′-TA TAT AAG CTT AGA TCT CCG GTC GGG TGC AGA CG-3′ (HindIII and BglII sites underlined) and cloned into pSP72, yielding pAL1082. These 1.5 kb XbaI/AflII and 1.2 kb HindIII/AflII fragments were respectively recovered from pAL1081 and pAL1082, and then ligated with a 0.5 kb EcoRI/XbaI fragment containing the *PermE** promoter in pSP72, yielding pAL1083, in which the 2.7 kb fragment encoding the N-terminal KS-AT domain of ChlB1 is under the control of the *PermE** promoter. On the other hand, a 1.0 kb PCR product encoding the DH domain was obtained by using the primers 5′-TA GAA TTC AGA TCT GGT CGC CCT GCC GCT G-3′ (EcoRI and BglII sites underlined) and 5′-TA TAT AAG CTT CCT AGG GTG CGC CGC CGT CAT G-3′ (AvrII site underlined) and cloned into pSP72, yielding pAL1084; a 1.9 kb fragment encoding the KR-ACP domain was obtained by using the primers 5′-TA GAA TTC CCT AGG GAC CTG GTC TTC GAG ATG-3′ (AvrII site underlined) and 5′-TA TAT AAG CTT TCA GGC CGT TGC CGC CGG-3′ (HindIII site underlined) and cloned into pSP72, yielding pAL1085. These 1.0 kb EcoRI/AvrII and 1.8 kb AvrII/HindIII fragments were respectively recovered from pAL1084 and pAL1085 and ligated into pSP72, yielding pAL1086, which contains the 2.9 kb fragment encoding the C-terminal DH-KR-ACP domain of ChlB1. Finally, the 3.2 kb EcoRI/BglII fragment from pAL1083 and 2.9 kb BglII/HindIII fragment from pAL1086 were recovered and cloned into pTGV2, yielding the recombinant construct pAL1087, in which *chlB1* is under the control of the *PermE** promoter.

To inactivate the DH domain of ChlB1 with pAL1084, which contains a 1.0 kb fragment encoding the DH domain as the template, PCR amplifications were carried out by using the primers 5′-C TAC CCC GGC AGC GCC ACC ATC AAC GGC ACG-3′ and 5′-CGT GCC GTT GAT GGT GGC GCT GCC GGG GTA G-3′ for mutation of H947 to A, and the primers 5′-C TAC CCC GGC AGC TTC ACC ATC AAC GGC ACG-3′ and 5′-CGT GCC GTT GAT GGT GAA GCT GCC GGG GTA G-3′ for mutation of H947 to F, at the conserved active site. To inactivate the KR domain of ChlB1 with pAL1085, which contains a 1.9 kb fragment encoding the KR-ACP domain as the template, PCR amplifications were carried out by using the primers 5′-C ACC GGC GGA CTG GCC ACC CTC GGC CTG G-3′ and 5′-C CAG GCC GAG GGT GGC CAG TCC GCC GGT G-3′ for mutation of G1389 to yield GxAxxG within the NADPH-binding motif, the primers 5′-C ACC GGC GCA CTG CCC ACC CTC GCC CTG G-3′ and 5′-C CAG GGC GAG GGT GGG CAG TGC GCC GGT G-3′ for mutation of G1387, G1389, and G1392 to yield AxPxxA, and the primers 5′-GGC CAG GCC GCC TTC GGC TCC GCC AAC G-3′ and 5′-C GTT GGC GGA GCC GAA GGC GGC CTG GCC-3′ for mutation of Y1540 to F at the conserved active site. Using the similar multiple-fragment ligation strategy described above, each mutant DNA fragment was assembled with the fragments encoding other functional domains, yielding the recombinant constructs pAL1088 for expressing the DH mutant ChlB1 (H947A), pAL1089 for expressing the DH mutant (H947F), pAL1090 for expressing the KR mutant (G1389A), pAL1091 for expressing the KR mutant (G1387A, G1389P, and G1392A), and pAL1092 for expressing the KR mutant (Y1540F).

Introduction of each plasmid DNA into *S. albus* was carried out by *E. coli-Streptomyces* conjugation following the procedure described previously

(Kieser et al., 2000). Colonies that were thiostrepton resistant were identified as the recombinant strains.

Production, Isolation, and Analysis of 6-MSA and OSA in *S. albus*

Fermentation of the *S. albus* strains and isolation and HPLC-MS analysis of their products were carried out according to the methods described previously (Shao et al., 2006; Zhao et al., 2008). The HR-EI-MS analyses were performed on a Waters Micromass GCT (monoisotopic mass, odd and even electron ions) mass spectrometer, establishing the molecular formulae as $C_8H_8O_3$ for 6-MSA (with the M^+ ion at m/z = 152.0477, 152.0473 calculated) and $C_8H_8O_4$ for OSA (with the M^+ ion at m/z = 168.0424, 168.0424 calculated). The standards OSA and TAL were purchased from Sigma-Aldrich.

Production, Isolation, and Analysis of Spirotetronates in *S. antibioticus*

Introduction of the recombinant plasmids pAL1092 encoding the KR mutant ChlB1 (Y1450F) and MSS4.3 encoding AviM into the *S. antibioticus* strain AL1012 (for DM-CHL production) was performed using the method described previously (Jia et al., 2006).

Fermentation of the *S. antibioticus* strains and isolation and HPLC-MS analysis of their products were carried out according to the methods described previously (Jia et al., 2006). NMR spectra for new spirotetronates **7** and **8**, along with CHL, were measured on a Bruker AV500/125 spectrometer (Supplemental Information). For **7**, ^{1}H and ^{13}C NMR assignments are listed in Table S2; HR-ESI-MS m/z $[M + Na]^+$ 959.40358 (calculated for $C_{50}H_{64}O_{17}Na^+$, 959.40412). For **8**, ^{1}H NMR (500 Hz, $CDCl_3$) δ 2.34 (s, 3H, 8′), 3.81 (s, 3H, 9′), 4.52 (d, J = 9.0 Hz, 1H, 1‴), 4.64 (d, J = 9.0 Hz, 1H, 1″), 5.02 (m, 1H, 3″), 5.17 (m, 1H, 17), 5.41 (m, 1H, 16), 5.59 (m, 1H, 10), 5.70 (d, J = 10.5 Hz, 1H, 9), 6.53 (s, 1H, 3′), 6.82 (brs, 1H, 19); and ^{13}C NMR (125 Hz, $CDCl_3$) δ 177.8 (C, 1), 47.7 (C, 2), 38.1 (CH, 3), 28.2 (CH_2, 4), 24.4 (CH_2, 5), 36.3 (CH_2, 6), 74.2 (CH, 7), 43.9 (CH, 8), 123.5 (CH, 9), 130.3 (CH, 10), 46.9 (CH, 11), 32.4 (CH_2, 12), 28.2 (CH_2, 13), 26.7 (CH_2, 14), 33.3 (CH_2, 15), 139.4 (CH, 16), 127.1 (CH, 17), 46.3 (CH, 18), 138.4 (CH, 19), 135.4 (C, 20), 27.2 (CH, 21), 35.2 (CH_2, 22), 80.6 (C, 23), 165.1 (C, 24), 124.4 (C, 25), 167.1 (C, 26), 17.4 (CH_3, 27), 172.6 (C, 28), 18.0 (CH_3, 29), 113.0 (C, 1′), 156.2 (C, 2′), 100.6 (CH, 3′), 153.5 (C, 4′), 116.7 (C, 5′), 135.4 (C, 6′), 159.6 (C, 7′), 100.6 (CH, 1″), 38.1 (CH_2, 2″), 74.9 (CH, 3″), 83.3 (CH, 4″), 72.2 (CH, 5″), 17.6 (CH_3, 6″), 101.3 (CH, 1‴), 28.6 (CH_2, 2‴), 70.2 (CH, 3‴), 88.6 (CH, 4‴), 70.2 (CH, 5‴), 17.0 (CH_3, 6‴); HR-ESI-MS m/z $[M + Na]^+$ 993.36460 (calculated for $C_{50}H_{63}O_{17}ClNa^+$, 993.36515).

In Vitro Susceptibility Testing

To detect the biological activities of spirotetronates against *S. subtilis* and *S. aureus*, 1, 2, 4, or 8 μg of each compound in 200 μl of methanol was added to stainless steel cylinders on Antibiotic Medium 2 (SCAS EcoScience Technology) agar plates that were preseeded with an overnight culture of the test strain at a concentration of 1% (vol/vol). The plates were incubated at 37°C for 24 hr, and the biological activity was estimated by measuring the sizes of the inhibition zones. All assays were carried out in triplicate.

To determine the minimum inhibitory concentrations (MICs), antibacterial activity was measured by broth dilution according to the method described previously (Pucci et al., 2004). Each test compound that was dissolved in dimethyl sulfoxide was diluted in water to produce a stock solution (256 μg/ml). Fifty microliters of the stock solution was serially diluted into Mueller-Hinton broth (Qingdao Hope Bio-Technology) in a 96-well microtiter plate. Fifty microliters of the test strain (~1.5×10^8 cfu/ml) was then added to each well of the microtiter plate. After incubation at 37°C for 18–24 hr, the MIC was determined to be the lowest concentration of compound that inhibited visible bacterial growth. All testing was carried out in duplicate.

SUPPLEMENTAL INFORMATION

Supplemental Information includes four figures and two tables and can be found with this article online at doi:10.1016/j.chembiol.2010.04.009.

ACKNOWLEDGMENTS

We thank Cesar Sanchez, Universidad de Oviedo, Spain, for providing *S. albus* J1047; Isao Fujii, University of Tokyo, for providing authentic 6-MSA; Andreas Bechthold, Universität Tübingen, for providing the construct MSS4.3; and Lei Shao, Shanghai Institute of Pharmaceutical Industry, for providing the test strains *B. subtilis* and *S. aureus*. This work was supported in part by grants from the National Natural Science Foundation of China (20832009, 30525001, 90713012, and 20921091), the Ministry of Science and Technology of China (2009ZX09501-008), the "973 Program" (2010CB833200), the Chinese Academy of Sciences (KJCX2-YW-H08 and KSCX2-YW-G-06), and the Science and Technology Commission of Shanghai Municipality (09QH1402700).

Received: November 23, 2009
Revised: March 31, 2010
Accepted: April 1, 2010
Published: May 27, 2010

REFERENCES

Ahlert, J., Shepard, E., Lomovskaya, N., Zazopoulos, E., Staffa, A., Bachmann, B.O., Huang, K., Fonstein, L., Czisny, A., Whitmam, R.E., et al. (2002). The calicheamicin gene cluster and its iterative type I enediyne PKS. Science *297*, 1173–1176.

Aparicio, J.F., Molnar, I., Schwecke, T., Konig, A., Haydock, S.F., Khaw, L.E., Staunton, J., and Leadlay, P.F. (1996). Organization of the biosynthetic gene cluster for rapamycin in *Streptomyces hygroscopicus*: analysis of the enzymatic domains in the modular polyketide synthase. Gene *169*, 9–16.

Balibar, C.J., Garneau-Tsodikova, S., and Walsh, C.T. (2007). Covalent CouN7 enzyme intermediate for acyl group shuttling in aminocoumarin biosynthesis. Chem. Biol. *14*, 679–690.

Beck, J., Ripka, S., Siegner, A., Schiltz, E., and Schweizer, E. (1990). The multifunctional 6-methylsalicylic acid synthase gene of *Penicillium patulum*: its gene structure relative to that of other polyketide synthases. Eur. J. Biochem. *192*, 487–498.

Bedford, D.J., Schweizer, E., Hopwood, D.A., and Khosla, C. (1995). Expression of a functional fungal polyketide synthase in the bacterium *Streptomyces coelicolor* A3(2). J. Bacteriol. *177*, 4544–4548.

Caffrey, P. (2003). Conserved amino acid residues correlating with ketoreductase stereospecificity in modular polyketide synthases. ChemBioChem *4*, 654–657.

Chen, Z., Lu, L., Shirley, M., Lee, W.R., and Chang, S.H. (1990). Site-directed mutagenesis of glycine-14 and two "critical" cysteinyl residues in *Drosophila* alcohol dehydrogenase. Biochemistry *29*, 1112–1118.

Crawford, J.M., Thomas, P.M., Scheerer, J.R., Vagstad, A.L., Kelleher, N.L., and Townsend, C.A. (2008). Deconstruction of iterative multidomain polyketide synthase function. Science *320*, 243–246.

Crawford, J.M., Korman, T.P., Labonte, J.W., Vagstad, A.L., Hill, E.A., Kamari-Bidkorpeh, O., Ysai, S.-H., and Townsend, C.A. (2009). Structural basis for biosynthetic programming of fungal aromatic polyketide cyclization. Nature *461*, 1139–1143.

Daum, M., Peintner, I., Linnenbrink, A., Frerich, A., Weber, M., Paululat, T., and Bechthold, A. (2009). Organisation of the biosynthetic gene cluster and tailoring enzymes in the biosynthesis of the tetracyclic quinone glycoside antibiotic polyketomycin. ChemBioChem *10*, 1073–1083.

Dimroth, P., Ringelmann, E., and Lynen, F. (1976). 6-methylsalicylic acid synthetase from *Penicillium patulum*. Some catalytic properties of the enzyme and its relation to fatty acid synthetase. Eur. J. Biochem. *68*, 591–596.

Freitag, A., Wemakor, E., Li, S., and Heide, L. (2005). Acyl transfer in chlorobiocin biosynthesis: involvement of several proteins in the transfer of the pyrrole-2-carboxyl moiety to the deoxysugar. ChemBioChem *6*, 2316–2325.

Fridman, M., Balibar, C.J., Lupoli, T., Kahne, D., Walsh, C.T., and Garneau-Tsodikova, S. (2007). Chemoenzymatic formation of novel aminocoumarin antibiotics by the enzymes CouN1 and CouN7. Biochemistry *46*, 8462–8471.

Fujii, I. (1999). Polyketide biosynthesis in filamentous fungi. In Comprehensive Natural Products Chemistry, Volume 1, U. Sankawa, ed. (Oxford: Elsevier), pp. 409–441.

Fujii, I., Ono, Y., Tada, H., Gomi, K., Ebizuka, Y., and Sankawa, U. (1996). Cloning of the polyketide synthase gene *atX* from *Aspergillus terreus* and its identification as the 6-methylsalicylic acid synthase gene by heterologous expression. Mol. Gen. Genet. *253*, 1–10.

Gaisser, S., Trefzer, A., Stockert, S., Kirschning, A., and Bechthold, A. (1997). Cloning of an avilamycin biosynthetic gene cluster from *Streptomyces viridochromogenes* Tü57. J. Bacteriol. *179*, 6271–6278.

He, Q., Jia, X., Tang, M., Tian, Z., Tang, G., and Liu, W. (2009). Dissection of two acyl-transfer reactions centered on acyl-S-carrier protein intermediates for incorporating 5-chloro-6-methyl-*O*-methylsalicyclic acid into chlorothricin. ChemBioChem *10*, 813–819.

Heide, L. (2009). Aminocoumarins mutasynthesis, chemoenzymatic synthesis, and metabolic engineering. Methods Enzymol. *459*, 437–455.

Hertweck, C. (2009). The biosynthetic logic of polyketide diversity. Angew. Chem. Int. Ed. Engl. *48*, 4688–4716.

Ito, T., Roongsawang, N., Shirasaka, N., Lu, W., Flatt, P.M., Kasanah, N., Miranda, C., and Mahmud, T. (2009). Deciphering pactamycin biosynthesis and engineering production of new pactamycin analogues. ChemBioChem *10*, 2253–2265.

Jia, X., Tian, Z., Shao, L., Qu, X., Zhao, Q., Tang, J., Tang, G., and Liu, W. (2006). Genetic characterization of the chlorothricin gene cluster as a model for spirotetronate antibiotic biosynthesis. Chem. Biol. *13*, 575–585.

Kawashima, A., Nakamura, Y., Ohta, Y., Akama, T., Yamagishi, M., and Hanada, K. (1992). New cholesterol biosynthesis inhibitors MC-031 (*O*-demethylchlorothricin), -032 (*O*-demethylhydroxychlorothricin), -033 and -034. J. Antibiot. (Tokyo) *45*, 207–212.

Kealey, J.T., Liu, L., Santi, D.V., Betlach, M.C., and Barr, P.J. (1998). Production of a polyketide natural product in nonpolyketide producing prokaryotic and eukaryotic hosts. Proc. Natl. Acad. Sci. USA *95*, 505–509.

Keatinge-Clay, A.T. (2007). A tylosin ketoreductase reveals how chirality is determined in polyketides. Chem. Biol. *14*, 898–908.

Keller-Schierlein, W., Muntwyler, R., Pache, W., and Zähner, H. (1969). Metabolic products of microorganisms. Chlorothricin and deschlorothricin. Helv. Chim. Acta *52*, 127–142.

Kennedy, J., Auclair, K., Kendrew, S.G., Park, C., Vederas, J.C., and Hutchinson, C.R. (1999). Modulation of polyketide synthase activity by accessory proteins during lovastatin biosynthesis. Science *284*, 1368–1372.

Kieser, T., Bibb, M.J., Butter, M.J., Chater, K.F., and Hopwood, D.A. (2000). Practical *Streptomyces* Genetics (Norwich, UK: The John Innes Foundation).

Ma, S.M., Li, J.W.-H., Choi, J.W., Zhou, H., Michael Lee, K.K., Moorthie, V.A., Xie, X., Kealey, J.T., Da Silva, N.A., Vederas, J.C., and Tang, Y. (2009). Complete reconstitution of a highly reducing iterative polyketide synthase. Science *326*, 589–592.

McDaniel, R., Welch, M., and Hutchinson, C.R. (2005). Genetic approaches to polyketide antibiotics. 1. Chem. Rev. *105*, 543–558.

Moriguchi, T., Ebizuka, Y., and Fujii, I. (2006). Analysis of subunit interactions in the iterative type I polyketide synthase ATX from *Aspergillus terreus*. ChemBioChem *7*, 1869–1874.

Moriguchi, T., Ebizuka, Y., and Fujii, I. (2008). Domain-domain interactions in the iterative type I polyketide synthase ATX from *Aspergillus terreus*. ChemBioChem *9*, 1207–1212.

Pucci, M.J., Bronson, J.J., Barrett, J.F., DenBleyker, K.L., Discotto, L.F., Fung-Tomc, J.C., and Ueda, Y. (2004). Antimicrobial evaluation of nocathiacins, a thiazole peptide class of antibiotics. Antimicrob. Agents Chemother. *48*, 3697–3701.

Reid, R., Piagentini, M., Rodriguez, E., Ashley, G., Viswanathan, N., Carney, J., Santi, D.V., Hutchinson, C.R., and McDaniel, R. (2003). A model of structure and catalysis for ketoreductase domains in modular polyketide synthases. Biochemistry *42*, 72–79.

Rescigno, M., and Perham, R.N. (1994). Structure of the NADPH-binding motif of glutathione reductase: efficiency determined by evolution. Biochemistry *33*, 5721–5727.

Richardson, M.T., Pohl, N.L., Kealey, J.T., and Khosla, C. (1999). Tolerance and specificity of recombinant 6-methylsalicylic acid synthase. Metab. Eng. *1*, 180–187.

Sambrook, J., and Russell, D.W. (2001). Molecular Cloning: A Laboratory Manual, Third Edition (Cold Spring Harbor, NY: Cold Spring Harbor Laboratory Press).

Schindler, P.W., and Zähner, H. (1972). Metabolic products of microorganisms. 96. Mechanism of action of the macrolide-type antibiotic, chlorothricin. I. Inhibitor of the pyruvate carboxylase from *Bacillus subtilis*. Arch. Mikrobiol. *82*, 66–75.

Shao, L., Qu, X., Jia, X., Zhao, Q., Tian, Z., Wang, M., Tang, G., and Liu, W. (2006). Cloning and characterization of a bacterial iterative type I polyketide synthase gene encoding the 6-methylsalicyclic acid synthase. Biochem. Biophys. Res. Commun. *345*, 133–139.

Shen, B. (2000). Biosynthesis of aromatic polyketides. Top. Curr. Chem. *209*, 1–51.

Singh, G.M., Vaillancourt, F.H., Yin, J., and Walsh, C.T. (2007). Characterization of SyrC, an aminoacyltransferase shuttling threonyl and chlorothreonyl residues in the syringomycin biosynthetic assembly line. Chem. Biol. *14*, 31–40.

Spencer, J.B., and Jordan, P.M. (1992). Purification and properties of 6-methylsalicylic acid synthase from *Penicillium patulum*. Biochem. J. *288*, 839–846.

Terekhova, L.P., Galatenko, O.A., Trenin, A.S., Tolstykh, I.V., Zenkova, V.A., Zhukhlistova, N.E., Ol'khovatova, O.L., Malkina, N.D., Boikova, L.V., Ustinova, E.V., and Katrukha, G.S. (2008). Isolation and study of antibiotic INA-1132 (chlorothricin), produced by actinomycete strain. Antibiot. Khimioter. *53*, 3–7.

Van Lanen, S.G., Dorrestein, P.C., Christenson, S.D., Liu, W., Ju, J., Kelleher, N.L., and Shen, B. (2005). Biosynthesis of the β-amino acid moiety of the enediyne antitumor antibiotic C-1027 featuring β-amino acyl-S-carrier protein intermediates. J. Am. Chem. Soc. *127*, 11594–11595.

Van Lanen, S.G., Oh, T.-J., Liu, W., Wendt-Pienkowski, E., and Shen, B. (2007). Characterization of the maduropeptin biosynthetic gene cluster from *Actinomadura madurae* ATCC 39144 supporting a unifying paradigm for enediyne biosynthesis. J. Am. Chem. Soc. *129*, 13082–13094.

Wu, J., Zaleski, T.J., Valenzano, C., Khosla, C., and Cane, D.E. (2005). Polyketide double bond biosynthesis. Mechanistic analysis of the dehydratase-containing module 2 of the picromycin/methymycin polyketide synthase. J. Am. Chem. Soc. *127*, 17393–17404.

Zhao, Q., He, Q., Ding, W., Tang, M., Kang, Q., Yu, Y., Deng, W., Zhang, Q., Fang, J., Tang, G., and Liu, W. (2008). Characterization of the azinomycin B biosynthetic gene cluster revealing a different iterative type I polyketide synthase for naphthoate biosynthesis. Chem. Biol. *15*, 693–705.